Biomaterials and Biosystems 6 (2022) 100049

Contents lists available at ScienceDirect

Biomaterials and Biosystems

journal homepage: www.elsevier.com/locate/bbiosy

Vascular tissue engineering from human adipose tissue: fundamental phenotype of its resident microvascular endothelial cells and stromal/stem cells

Jeremy A. Antonyshyn[a,b], Meghan J. McFadden[a,b], Anthony O. Gramolini[b,c], Stefan O.P. Hofer[d,e], J. Paul Santerre[a,b,f,*]

[a] Institute of Biomedical Engineering, University of Toronto, Toronto, Canada
[b] Translational Biology and Engineering Program, Ted Rogers Centre for Heart Research, Toronto, Canada
[c] Department of Physiology, University of Toronto, Toronto, Canada
[d] Division of Plastic, Reconstructive, and Aesthetic Surgery, University of Toronto, Toronto, Canada
[e] Departments of Surgery and Surgical Oncology, University Health Network, Toronto, Canada
[f] Faculty of Dentistry, University of Toronto, Toronto, Canada

ARTICLE INFO

Keywords:
Vascular tissue engineering
Adipose tissue
Endothelial cell
Adipose tissue-derived stromal/stem cell
Endothelial progenitor cell
Proteomics

ABSTRACT

Adipose tissue is an abundant, accessible, and uniquely dispensable source of cells for vascular tissue engineering. Despite its intrinsic endothelial cells, considerable effort is directed at deriving endothelium from its resident stem and progenitor cells. Here, we investigate the composition of human adipose tissue and characterize the phenotypes of its constituent cells in order to help ascertain their potential utility for vascular tissue engineering. Unsupervised clustering based on cell-surface protein signatures failed to detect $CD45^{-}CD31^{-}VEGFR2^{+}$ endothelial progenitor cells within adipose tissue, but supported further investigation of its resident $CD45^{-}CD31^{+}$ microvascular endothelial cells (HAMVECs) and $CD45^{-}CD31^{-}$ stromal/stem cells (ASCs). The endothelial differentiation of ASCs altered their proteome, but it remained distinct from that of primary endothelial cell controls – as well as HAMVECs – regardless of their arterial-venous specification or macrovascular-microvascular origin. Rather, ASCs retained a proteome indicative of a perivascular phenotype, which was supported by their ability to facilitate the capillary morphogenesis of HAMVECs. This study supports the use of HAMVECs for the generation of endothelium. It suggests that the utility of ASCs for vascular tissue engineering lies in their capacity to remodel the extracellular matrix and to function as mural cells.

Introduction

Fat is an attractive resource for tissue engineering. It is an abundant and uniquely dispensable tissue that can be readily harvested with minimally invasive procedures; in fact, fat is routinely aspirated for cosmetic indications, after which it is either discarded as waste or used to augment the volume of soft tissues elsewhere on the body [1,2]. It is therefore pertinent to envision fat being repurposed for therapeutic indications, in a process by which it is harvested and disassembled into its cellular constituents that can then be used as building blocks for tissue engineering in an autologous, patient-specific manner. Of particular importance to the survival and function of engineered tissues is the inclusion of vascular networks that can integrate into the host's circulatory system [3].

Comprising a single layer of cells lining the luminal surface of the vasculature, the endothelium is the interface between blood and the different tissues of the body [4]. It is not a passive barrier, but actively regulates hemostasis, perfusion, and inflammation [4]. Endothelial cells (ECs) are consequently indispensable for the construction of vasculature. Remarkably, effort continues to be primarily directed at deriving endothelium from adipose tissue-resident stem and progenitor cells [5–16], despite the existence of natively differentiated ECs within its stromal vascular fraction [17–21].

We have previously described the strikingly limited endothelial plasticity of adipose tissue-derived stromal/stem cells (ASCs) [22], and have more recently demonstrated the feasibility of isolating human adipose tissue-derived microvascular ECs (HAMVECs) in large quantities with high purity [18]. HAMVECs exhibit morphological, molecular, and functional hallmarks of endothelium [18], while the endothelial differentiation of ASCs using well-established biochemical stimuli fails to induce in them these characteristic endothelial traits [22]. However, the paucity of markers with specificity and sensitivity for the endothelial lin-

* Corresponding author.
E-mail address: paul.santerre@utoronto.ca (J.P. Santerre).

https://doi.org/10.1016/j.bbiosy.2022.100049
Received 23 January 2022; Received in revised form 19 March 2022; Accepted 10 April 2022

eage challenges their dismissal for the generation of endothelium [23]. In fact, the endothelium exhibits marked phenotypic heterogeneity between vascular beds in order to fulfill the distinct requirements of the different vessels and tissues that it services [4,23]. Not only does this suggest that ASCs may in fact be capable of functioning as endothelium for specialized indications, but it also suggests that the utility of HAMVECs for vascular tissue engineering may be favourable for others.

Here, we investigate the composition of human adipose tissue and characterize the phenotypes of its constituent cells in order to help ascertain their potential utility for vascular tissue engineering (**Supplementary Fig. 1**). The composition of the stromal vascular fraction of human subcutaneous abdominal white adipose tissue was probed by flow cytometry. Magnet-assisted cell sorting was used to isolate HAMVECs and ASCs, and the endothelial differentiation of the latter was induced using media supplemented with vascular endothelial growth factor (VEGF) and basic fibroblast growth factor (bFGF). The proteomes of HAMVECs and ASCs were then compared with controls representative of the predominant endothelial specializations, and their putative phenotypes were corroborated by tracing their spontaneous self-assembly into microvascular-like networks in both gelled basement membrane extract and co-culture. Our findings support the use of HAMVECs for the vascularization of engineered tissues [3] and the endothelialization of small diameter vascular prostheses [24], and suggest that the utility of ASCs for vascular tissue engineering lies in their capacity to remodel the extracellular matrix and to function as mural cells.

Materials and methods

Materials

Subcutaneous abdominal white adipose tissue was obtained with informed consent from patients presenting for reconstructive breast surgery at the University Health Network (Toronto, Ontario, Canada; institutional research ethics board approval no. 13-6437-CE). Tissue culture-treated polystyrene (TCPS) was sourced from Corning (Corning, New York, United States). Unless indicated otherwise, all other materials were from MilliporeSigma (St. Louis, Missouri, United States).

Isolation of the stromal vascular fraction

The stromal vascular fraction was harvested from enzymatically digested adipose tissue as previously described [18,22]. Briefly, adipose tissue was minced and enzymatically digested for 1 h at 37 °C using collagenase type II (2 mg/mL) in Kreb's Ringer bicarbonate buffer supplemented with 3 mM glucose, 25 mM 4-(2-hydroxyethyl)-1-piperazineethanesulfonic acid, and 20 mg/mL bovine serum albumin (BSA). The buoyant adipocytes were discarded following the centrifugation of the digest, and the pelleted tissue was subjected to another 15 min of enzymatic digestion at 37 °C using 0.25% trypsin-ethylenediaminetetraacetic acid (EDTA) solution. The cells were then resuspended in sterile distilled and deionized water supplemented with 0.154 M ammonium chloride, 10 mM potassium bicarbonate, and 0.1 mM EDTA for 10 min to facilitate erythrocyte lysis, before being filtered through 100 μm and 40 μm sieves, sequentially. The resulting filtrate comprised the stromal vascular fraction and was immediately prepared for flow cytometry or magnet-assisted cell sorting.

Flow cytometry

The stromal vascular fraction ($N = 3$ biologically independent samples) was stained with Live/Dead Fixable Aqua (Invitrogen, Carlsbad, California, United States), blocked using Human TruStain FcX (BioLegend, San Diego, California, United States), and then stained for 20 min at 4°C with the following fluorophore-conjugated mouse anti-human monoclonal antibodies (BioLegend): CD45-APC/Cy7 (catalogue no. 368516), CD14-PE/Cy7 (catalogue no. 367112), CD34-PE/Dazzle 594 (catalogue no. 343534), CD31-Alexa Fluor 488 (catalogue no. 303110), and vascular endothelial growth factor receptor 2 (VEGFR2; CD309; *KDR*)-Alexa Fluor 647 (catalogue no. 359910). Stained cells were fixed with 4% (w/v) paraformaldehyde in phosphate-buffered saline (without calcium chloride and magnesium chloride; $PBS^{-/-}$) for 15 min at 4°C. Compensation was achieved using the AbC Anti-Mouse Bead Kit and the ArC Amine Reactive Compensation Bead Kit (Invitrogen). Gates were set using fluorescence minus one (FMO) controls (**Supplementary Fig. 2**). Flow cytometry was performed using a BD LSR II (Becton, Dickinson and Company, Franklin Lakes, New Jersey, United States) at the Temerty Faculty of Medicine Flow Cytometry Facility (University of Toronto, Toronto, ON, Canada). Data was acquired using BD FACSDiva software version 8.0.1 (Becton, Dickinson and Company), and analyzed using FlowJo software version 10.8.1 (Becton, Dickinson and Company).

Cell culture

$CD45^-CD31^-$ ASCs (N = 3 biologically independent samples) and $CD45^-CD31^+$ HAMVECs (N = 3 biologically independent samples) were isolated from the stromal vascular fraction using magnet-assisted cell sorting [18,22]. Human umbilical vein ECs (HUVECs; Lonza, Walkersville, Maryland, United States; $N = 3$ biologically independent samples), human coronary artery ECs (HCAECs; Lonza; $N = 3$ biologically independent samples), and human dermal microvascular ECs (HDMVECs; Lonza and PromoCell, Heidelberg, Baden-Württemberg, Germany; $N = 3$ biologically independent samples) were obtained commercially from three different donors each.

All cells were cultured on TCPS and maintained at 37 °C, 5% CO_2 under a relative humidity of 85%. ASCs were cultured in Dulbecco's Modified Eagle Medium and Ham's F-12 nutrient mixture (DMEM:F12) supplemented with 10% (v/v) fetal bovine serum, 100 U/mL penicillin, and 0.1 mg/mL streptomycin; and, ECs were cultured in Endothelial Cell Growth Medium-2 (EGM2; Lonza). The endothelial differentiation of ASCs was induced by their culture in EGM2 for 14 days [22]. For all cells, media was exchanged three times a week and cells were passaged at 75 – 90% confluence using TrypLE Express (Invitrogen). Phase-contrast transmission light microscopy was used to assess morphology and confluence (Leica DMIL, Leica Microsystems, Wetzlar, Hesse, Germany). Cells were counted using a hemocytometer, and dead cells were excluded on the basis of trypan blue staining.

Liquid chromatography – tandem mass spectrometry

Reversed-phase liquid chromatography – tandem mass spectrometry (LC-MS/MS) was performed as previously described [18,22]. Briefly, cell lysate-derived tryptic peptides were analyzed on an Easy-nLC 1200 (Thermo Fisher Scientific, Waltham, Massachusetts, United States) coupled to a Q Exactive Plus mass spectrometer (Thermo Fisher Scientific) through a Nanospray Flex Ion Source (Thermo Fisher Scientific). All experiments utilized two technical replicates for each biological sample, and spectra were collected using a top 10 data-dependent acquisition method. Raw files were searched against the UniProt human proteome database (updated to 2017-07-24) using MaxQuant software version 1.6.0.1 (Max Planck Institute of Biochemistry, Planegg, Bavaria, Germany) [25]. Cysteine carbamidomethylation was set as a fixed modification, and methionine oxidation, N-terminal acetylation, and asparagine or glutamine deamidation were selected as variable modifications. The false discovery rate (FDR) was set to 1% using a reversed-target decoy database. Raw data are available from the MassIVE repository (accession no. MSV000086982), and the corresponding tabulated data set of the search results are available in **Supplementary Data 1**.

Unless indicated otherwise, data visualization and statistical analyses were completed using the Perseus 1.6.15.0 software package (Max Planck Institute of Biochemistry) [26]. Label-free quantification (LFQ) values were $\log_2$-transformed [27], and missing values were imputed

from a normal distribution using a downshift of 1.8 and width of 0.3 standard deviations (**Supplementary Data 1**). Principal component analysis was performed on $\log_2$-transformed LFQ values of proteins that were detected in ≥ 2 biological replicates in at least one group. The distribution of proteins detected in ≥ 2 biological replicates per group was assessed using the UpSetR package version 1.4.0 in RStudio version 2021.9.1.372 [28,29]. Unsupervised hierarchical clustering and the associated heat map of differentially expressed proteins between groups (FDR < 0.05) was generated from their Z-scores (normalized across all samples for each protein), and clusters of proteins were defined using a resolution of 6. Gene ontological enrichment analyses of the clusters was performed using an adapted procedure [30]. Briefly, statistically overrepresented (FDR < 0.05) biological pathways (GO Ontology database; DOI:10.5281/zenodo.5228828; released 2021-08-18), among the differentially expressed proteins comprising each cluster, were identified using Fisher's Exact test within PANTHER version 16.0 (released 2021-02-24) [31], and redundant gene ontology (GO) terms were eliminated using REVIGO based on a dispensability cut-off of < 0.05 (**Supplementary Data 2**) [32]. These truncated lists of statistically overrepresented (FDR < 0.05) GO biological processes were plotted using an adapted script within the ggplot2 package version 3.3.5 in RStudio version 2021.9.1.372[30]. Finally, a heat map of select differentially expressed proteins (FDR < 0.05) was generated using Prism 9 software version 9.2.0 (GraphPad Software, San Diego, California, United States), based on their Z-scores normalized across all samples for each protein.

Capillary morphogenesis in gelled basement membrane extract

The angiogenic capacity of HAMVECs and ASCs in gelled basement membrane extract was assessed [18,33]. Briefly, cells were seeded at a density of 45,000 cells/cm^2 onto TCPS coated with 150 μL/cm^2 of Cultrex PathClear Basement Membrane Extract (Bio-Techne, Minneapolis, Minnesota, United States). After 6 hr of culture in EGM2, their formation of microvascular-like networks was assessed using phase-contrast transmission light microscopy (Leica DMIL).

Capillary morphogenesis in co-culture

The morphogenesis of HAMVECs and ASCs in co-culture was assessed. HAMVECs and ASCs were seeded in a 1:1 proportion amounting to a total cell seeding density of 200,000 cells/cm^2 onto 35 mm μ-Dishes (ibidi GmbH, Gräfelfing, Germany). In one iteration, HAMVECs were labelled with 10 μM CellTrace Far Red (Invitrogen) to facilitate their discrimination from ASCs. After 7 days in culture in EGM2 (**Supplementary Fig. 3**), cells were rinsed with phosphate-buffered saline (with calcium chloride and magnesium chloride; PBS$^{+/+}$) before being fixed and permeabilized with either ice-cold methanol for 10 min at –20 °C, or with 4% (w/v) paraformaldehyde in PBS$^{-/-}$ for 15 min at 25 °C followed by 0.1% (v/v) Triton X-100 in PBS$^{-/-}$ for 15 min at 25 °C. Cells were then blocked with 3% (w/v) BSA in PBS$^{-/-}$ for 30 min, and stained overnight at 4 °C in 3% (w/v) BSA in PBS$^{-/-}$ supplemented with 5 μg/mL of both mouse anti-human CD31 primary antibody (AbCam, Cambridge, United Kingdom; catalogue no. ab24590) and rabbit anti-human α-smooth muscle actin (αSMA) primary antibody (AbCam; catalogue no. ab5694). Cells were rinsed with PBS$^{-/-}$, blocked using Normal Serum Block (BioLegend) for 30 min at 25 °C, and then stained for 1 h in 3% (w/v) BSA in PBS$^{-/-}$ supplemented with 2.5 μg/mL of both goat anti-mouse IgG-Alexa Fluor 555 secondary antibody (Cell Signaling Technology, Danvers, Massachusetts, United States; catalogue no. 4409S) and goat anti-rabbit IgG-Alexa Fluor 647 secondary antibody (Cell Signaling Technology; catalogue no. 4414S) or goat anti-rabbit IgG-Alexa Fluor 488 secondary antibody (Cell Signaling Technology; catalogue no. 4412S). Cells were then counterstained for 5 min with 3 μM 4′,6-diamidino-2-phenylindole (DAPI; AbCam) in PBS$^{-/-}$. Images were acquired using a Leica SP8 confocal scanning laser microscope (Leica Microsystems) at the Advanced Optical Microscopy Facility (University Health Network), and processed using Fiji version 2.3.0/1.53f [34].

Statistical analyses

All experiments were performed in biological triplicate, using cells derived from three different donors (N = 3 biologically independent samples). Where applicable, statistical analyses were described along with their respective experiments. Unless indicated otherwise, values are represented as mean ± standard deviation.

Results

Fat is a source of endothelial cells and perivascular cells for vascular tissue engineering, but not endothelial progenitor cells

Adipose tissue comprises a heterogeneous mixture of cells (**Fig. 1**). Encompassing all but the adipocytes, its stromal vascular fraction can be conceptualized as being composed of three principal populations: vascular (HAMVECs), perivascular (ASCs), and hematopoietic (leukocytes; **Fig. 1a**). They can be discerned based on their expression of the pan-hematopoietic marker CD45 and the pan-endothelial marker CD31 (**Fig. 1b**). CD45$^-$CD31$^+$ HAMVECs comprise 1.3 ± 0.5% of the stromal vascular fraction; CD45$^-$CD31$^-$ ASCs, 56.1 ± 3.1%; and, CD45$^+$ leukocytes, 42.5 ± 3.4% (**Fig. 1c**). While their unsupervised clustering failed to detect a distinct subpopulation of CD45$^-$CD31$^-$VEGFR2$^+$ endothelial progenitor cells (EPCs), two subpopulations of perivascular cells were identified: CD45$^-$CD31$^-$CD34$^-$ ASCs and CD45$^-$CD31$^-$CD34$^+$ ASCs (**Fig. 1a, b**). These findings support the utility of fat as a source of cells for vascular tissue engineering, but also suggest that effort is better directed towards investigating the regenerative potential of its resident HAMVECs and ASCs than searching for an elusive subpopulation of EPCs.

Adipose tissue-derived stromal/stem cells stimulated with VEGF and bFGF do not assume an endothelial proteome, but retain markers of a perivascular phenotype

The proteomes of HAMVECs and ASCs were assessed to help ascertain their utility for vascular tissue engineering (**Fig. 2**). CD45$^-$CD31$^+$ HAMVECs and CD45$^-$CD31$^-$ ASCs were isolated with purities of 98.6 ± 0.9% and 99.8 ± 0.2%, respectively. The endothelial differentiation of ASCs was induced through their culture in medium containing VEGF and bFGF. HAMVECs and ASCs were then compared to EC controls derived from different vascular beds, namely the umbilical vein (HUVECs), coronary artery (HCAECs), and dermis (HDMVECs).

The endothelial differentiation of ASCs altered their proteome, but it remained distinct from that of ECs – including HAMVECs (**Fig. 2a**). The endothelial differentiation of ASCs induced in them a significant change in two main clusters of proteins (Clusters I & VI; **Fig. 2c, d**). However, gene ontological analyses of these differentially expressed proteins revealed that the statistically overrepresented biological processes were limited to metabolism (GO accession no. GO:0008152 & GO:0019752; **Fig. 2e**), suggesting that the stimulation of ASCs with VEGF and bFGF does not induce in them a marked phenotypic change.

The distinct phenotypes of ECs and ASCs was underscored by their unsupervised hierarchical clustering, in which pervasive patterns in their protein expression profiles readily distinguished between the two cell types (**Fig. 2c**). Of the 1,431 proteins detected in different abundances between any groups of cells, 82% were differentially expressed between ECs and ASCs (Clusters II & III; **Fig. 2c, d**). Biological processes implicated in endothelial development were enriched in ECs (GO accession no. GO:0003158; Cluster III; **Fig. 2c – e**), whereas biological processes related to cytoskeletal structure and extracellular matrix remodeling were enriched in ASCs (GO accession no. GO:0030029, GO:0032970, GO:0030199, GO:1902903, & GO:1905049; Cluster II; **Fig. 2c – e**).

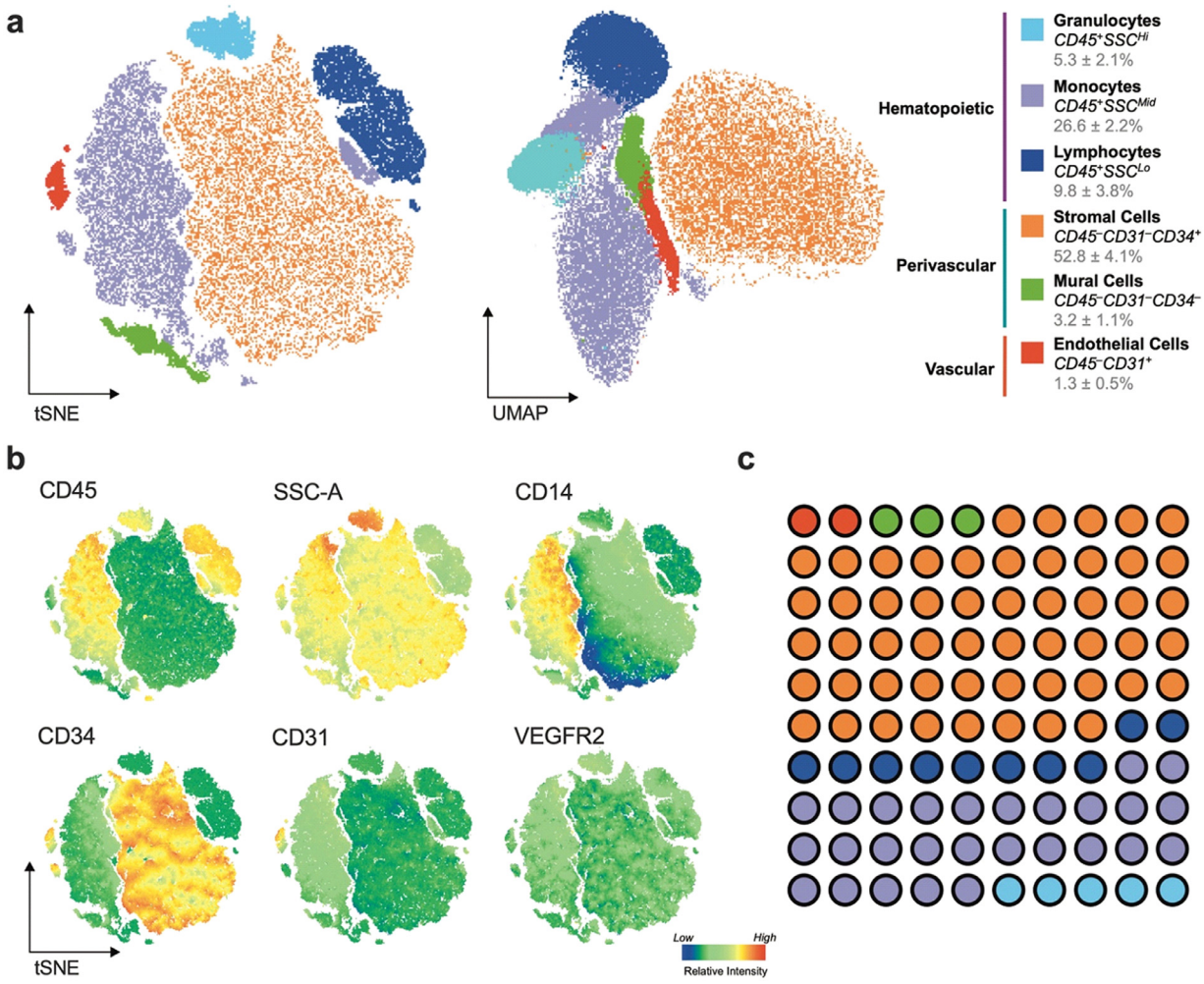

Fig. 1. Adipose tissue is a source of endothelial cells and perivascular cells for vascular tissue engineering, not endothelial progenitor cells. (**a**) Composition of the stromal vascular fraction of enzymatically digested fat. Shown are a t-distributed stochastic neighbour embedding (t-SNE) plot and a uniform manifold approximation and projection (UMAP) plot depicting the unsupervised clustering of stromal vascular cells based on their cell-surface protein signatures detected by flow cytometry. (**b**) Heat maps depicting the relative expression of the markers used to identify the different populations of cells. (**c**) Waffle chart depicting the proportions of the different populations of cells within the stromal vascular fraction of fat. This experiment was performed using cells derived from three different donors ($N = 3$ biologically independent samples).

These findings support the endothelial phenotype of HAMVECs, and suggest that ASCs retain a perivascular phenotype despite their stimulation with VEGF and bFGF.

Closer examination of the proteins differentiating HAMVECs and ASCs helped elucidate their utility of vascular tissue engineering (Fig. 2**f**). HAMVECs were enriched for endothelial transcription factors (*ERG, EDF1, NR2F2*), as well as their downstream proteins implicated in maintaining the endothelial barrier (*PECAM1, CDH5, TJP2, F11R, CTNNB1*) and its hemostatic properties (*VWF, MMRN1, CD59, TFPI*). In contrast, ASCs were enriched for proteins involved in mural cell development (*NOTCH2, PDGFRB, LRP1*), contractility (*CALD1, CNN3, TAGLN, ATP2B1, TGFB1I1*), and remodelling of the extracellular matrix (*TGFBI, SERPINH1, RECK, TIMP1, TIMP3*). Furthermore, while ASCs expressed fibronectin (*FN1*) and a number of interstitial collagens, HAMVECs were enriched for constituents of the endothelial basement membrane – namely, nidogen (*NID1*), perlecan (*HSPG2*), collagen IV (*COL4A1, COL4A2*), collagen XVIII (*COL18A1*), and laminin (*LAMA4, LAMB1*). Notably, laminins are heterotrimeric proteins comprising α-, β-, and γ-chains. Although HAMVECs exhibited an abundance of certain isoforms of the α- and β-chains (*LAMA4, LAMB1*), ASCs were enriched for other isoforms of the β- and γ-chains (*LAMB2, LAMC1*). Moreover, ASCs were enriched for heat shock protein 47 (Hsp47; *SERPINH1*), which is implicated in the assembly of collagen IV. While these findings support the use of HAMVECs for the generation of endothelium, they suggest that ASCs may be important for the stabilization and maturation of the endothelium – in part, by facilitating the assembly of its basement membrane.

Human adipose tissue-derived microvascular endothelial cells do not exhibit any readily apparent limitations on their utility for vascular tissue engineering

Although the endothelial phenotype of HAMVECs is clear (Fig. 2), the endothelium exhibits marked heterogeneity between vascular beds in order to fulfill the distinct requirements of the different vessels and tissues that it services. This phenotypic heterogeneity was manifested in the proteomes of the ECs, in which their principal component analysis effectively grouped ≥ 2 biological replicates from each of the four different vascular beds investigated (Fig. 2**a**). HUVECs exhibited the most distinctive proteome (Fig. 2**b, c**), with biological processes implicated in immunity being statistically overrepresented among its differentially expressed proteins (GO accession no. GO:0002376, GO:0031347, & GO:0034341; Cluster V; Fig. 2**c – e**). Specifically, HUVECs exhibited lower levels of immune markers, including those implicated in process-

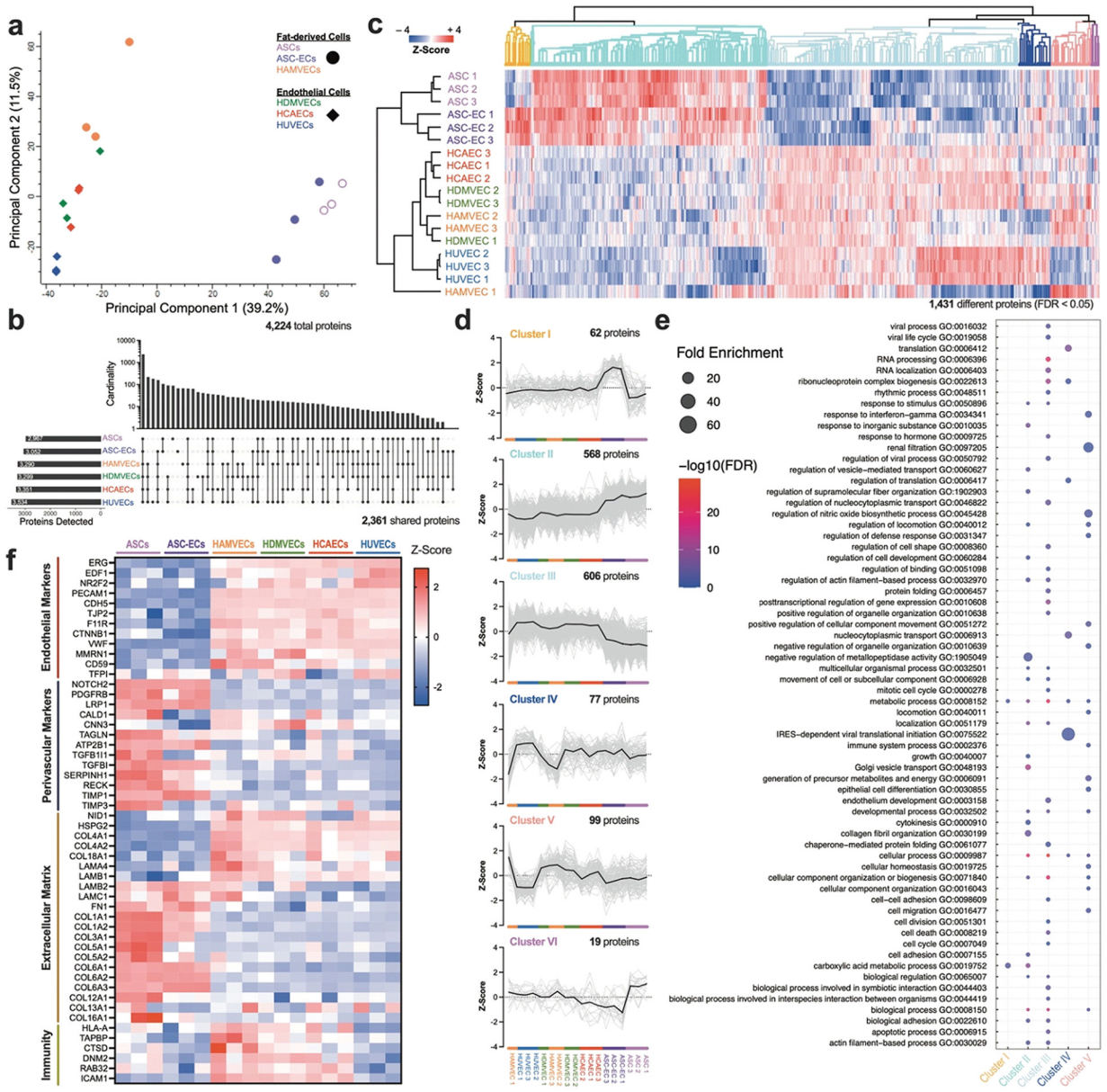

Fig. 2. Adipose tissue-derived stromal/stem cells (ASCs) stimulated with vascular endothelial growth factor (VEGF) and basic fibroblast growth factor (bFGF) do not assume an endothelial proteome such as that of human adipose tissue-derived microvascular endothelial cells (HAMVECs), but retain markers of a perivascular phenotype. ASCs and HAMVECs were isolated from the stromal vascular fraction of enzymatically digested fat. The endothelial differentiation of ASCs (ASC-ECs) was induced through their culture in medium containing VEGF and bFGF for 14 days. Liquid chromatography – tandem mass spectrometry (LC-MS/MS) was used to compare the proteomes of ASCs, ASC-ECs, and HAMVECs with endothelial cell (EC) controls representative of the predominant endothelial specializations, namely human umbilical vein ECs (HUVECs; macrovascular, venous endothelium), human coronary artery ECs (HCAECs; macrovascular, arterial endothelium), and human dermal microvascular ECs (HDMVECs; microvascular endothelium). (**a**) Principal component analysis of their global proteomes. (**b**) UpSet plot depicting the distribution of detected proteins amongst the different groups of cells. (**c**) Unsupervised hierarchical clustering and heat map of the differentially expressed proteins (FDR < 0.05). (**d**) Profile plots of the clusters of differentially expressed proteins. Gray lines depict individual proteins; and, black, the mean. (**e**) Gene ontological (GO) enrichment analysis of the clusters. Shown are the statistically overrepresented (FDR < 0.05) biological processes. None were detected for cluster VI. (**f**) Heat map depicting the relative abundance of select differentially expressed proteins (FDR < 0.05). This experiment was performed using cells derived from three different donors for each cell type ($N = 3$ biologically independent samples).

ing and presenting self-antigen (*HLA-A, TAPBP, CTSD, DNM2, RAB32, ICAM1*; Fig. 2**f**). HAMVECs expressed lower abundances of proteins involved in translation when compared with the other ECs (GO accession no. GO:0006412, GO:0006417, GO:0006913, & GO:0022613; Cluster IV; Fig. 2**c – e**), but they exhibited no readily apparent limitations on their barrier nor hemostatic properties (Fig. 2**f**); that is, despite their phenotypic heterogeneity between vascular beds, all ECs expressed comparable levels of proteins responsible for maintaining blood in a fluid state and confining its flow to the boundaries of the vessels.

Adipose tissue-derived stromal/stem cells support the capillary morphogenesis of human adipose tissue-derived microvascular endothelial cells

The self-assembly of ECs into microvascular-like networks is a hallmark of their endothelial phenotype. Despite their distinct proteomes (Fig. 2), both HAMVECs and ASCs readily formed tubular networks on gelled basement membrane extract (Fig. 3**b**). While co-culturing HAMVECs and ASCs in the absence of this substrate also resulted in

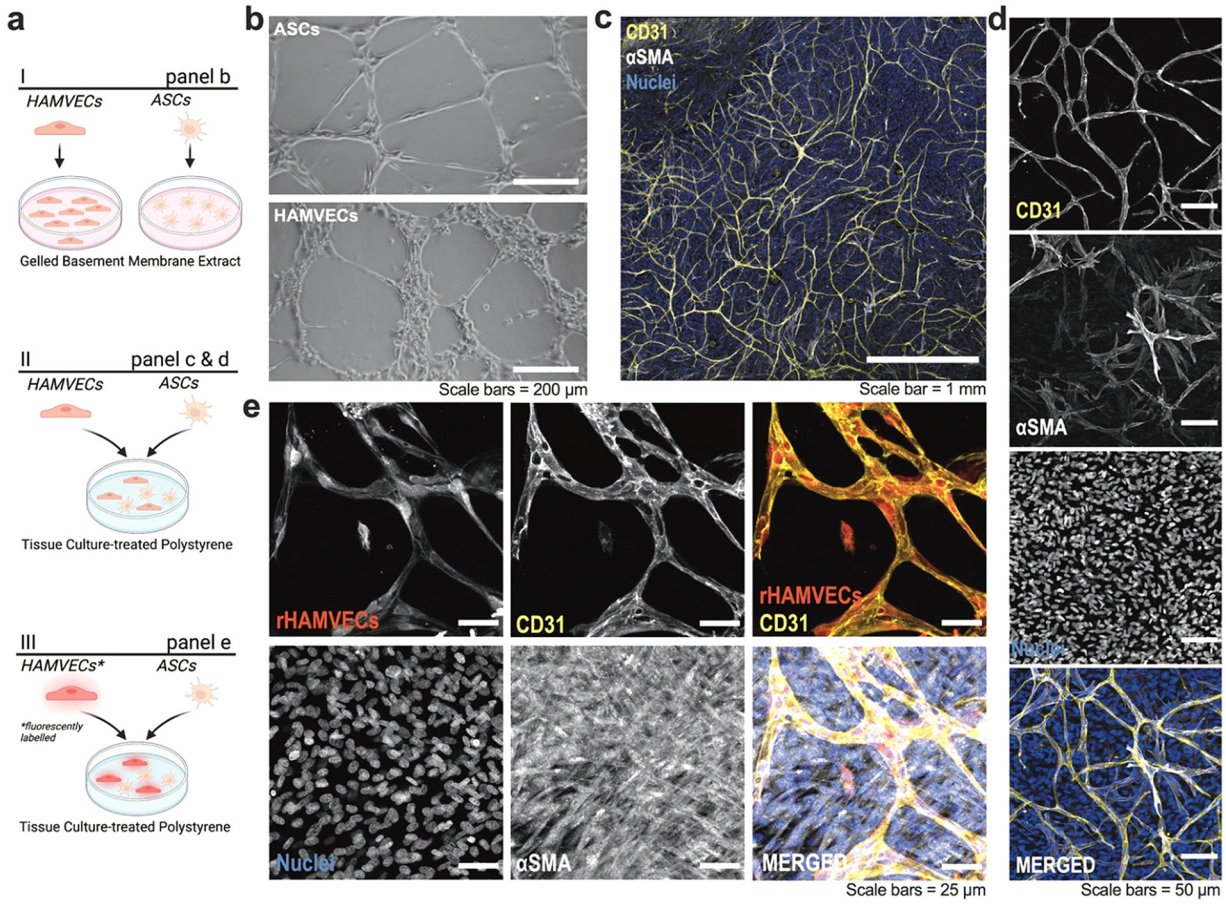

Fig. 3. Adipose tissue-derived stromal/stem cells (ASCs) support the capillary morphogenesis of human adipose tissue-derived microvascular endothelial cells (HAMVECs). (**a**) Schematic illustrating the workflow used to assess the spontaneous self-assembly of HAMVECs and ASCs in both (I) gelled basement membrane extract and (II – III) co-culture. (**b**) Capillary morphogenesis of HAMVECs and ASCs in gelled basement membrane extract after 6 hours of culture. (**c**) Capillary morphogenesis within co-cultures of HAMVECs and ASCs after 7 days. (**d**) Expression and localization of α-smooth muscle actin (αSMA) in co-cultures of HAMVECs and ASCs after 7 days. (**e**) Localization of fluorescently labelled HAMVECs (rHAMVECs) in co-culture with ASCs after 7 days. All experiments were performed using cells derived from three different donors ($N = 3$ biologically independent samples). Depicted are representative photomicrographs obtained by phase-contrast transmission light microscopy (**b**), and representative maximum intensity projections obtained by z-stacking confocal scanning laser microscopy (**c – e**).

their spontaneous self-assembly into extensive microvascular-like networks (Fig. 3**c**), fluorescent cell tracing demonstrated that these vessels were composed of HAMVECs – not ASCs, nor a subpopulation thereof (e.g. EPCs; Fig. 3**e**). Interestingly, however, two subpopulations of ASCs could be discerned based on their expression of the mural cell marker αSMA (Fig. 3**d**). Although most ASCs exhibited diffuse αSMA expression, a small proportion exhibited well-defined αSMA filaments (Fig. 3**d**). The latter were in close proximity to the vasculature, particularly at their branches (Fig. 3**d**). These findings support the use of HAMVECs, and not ASCs, for the generation of endothelium. They demonstrate that ASCs stimulated with VEGF and bFGF retain their perivascular phenotype, and suggest that their utility for vascular tissue engineering lies in their capacity to support HAMVECs.

Discussion

Adipose tissue is an attractive source of cells for vascular tissue engineering because it can be harvested in large quantities with minimally invasive procedures [1,2]. Despite its intrinsic ECs [17–21], considerable effort is directed at deriving endothelium from its resident stem and progenitor cells [5–16]. Here, we demonstrate that the utility of ASCs for vascular tissue engineering resides not in their phenotypic plasticity, but in their perivascular phenotype and capacity to support HAMVECs.

While we have previously demonstrated the feasibility of isolating $CD45^{-}CD31^{+}$ HAMVECs [18] and described the limited endothelial plasticity of $CD45^{-}CD31^{-}$ ASCs [22], many have attempted to derive endothelium from a putative subpopulation of the latter, namely EPCs [13–15]. In contrast to the $CD45^{-}CD31^{+}$ cell-surface protein signature indicative of differentiated endothelium, EPCs are developmentally characterized by a $CD45^{-}CD31^{-}VEGFR2^{+}$ immunophenotype [35–37]. Unsupervised clustering of stromal vascular cells based on their cell-surface protein signatures failed to detect a distinct $CD45^{-}CD31^{-}VEGFR2^{+}$ subpopulation (Fig. 1), contesting the persistence of developmentally conserved EPCs within fat. Rather, previous investigations of EPCs have isolated the cells from fat on the basis of a $CD34^{+}$ immunophenotype [14,15]. CD34 is co-expressed by 94.2 ± 2.2% of $CD45^{-}CD31^{-}$ ASCs (Fig. 1), suggesting that these studies may have unintentionally investigated ASCs rather than a subpopulation of EPCs with enhanced plasticity for the endothelial lineage. Nevertheless, considerable effort continues to be directed at differentiating ASCs into ECs [5–16], warranting a critical assessment of their phenotype.

The endothelial differentiation of ASCs was induced using media supplemented with VEGF and bFGF. Not only are these growth factors implicated in the differentiation and survival of ECs [38], but this biochemical stimulation is also the most commonly used method described in the literature for inducing the endothelial differentiation of ASCs [5,7–9,11–13,16]. Although other microenvironmental cues such as shear stress

[16], substrate topography [7], and three-dimensional culture [8] have been reported to potentiate their upregulation of characteristic endothelial markers, we have previously demonstrated that the magnitudes of these upregulations are negligible when compared with the levels of expression observed in ECs – which are orders of magnitude higher than in ASCs [22]. Here, we build upon our previous observations and demonstrate that despite their stimulation with VEGF and bFGF, ASCs do not assume an endothelial phenotype, but rather retain a proteomic signature indicative of a perivascular phenotype (**Fig. 2**).

Despite their distinct proteomes, both HAMVECs and ASCs spontaneously self-assemble into microvascular-like networks on gelled basement membrane extract (**Fig. 3**). While this capillary morphogenesis of ASCs is often cited as evidence of their successful endothelial differentiation [6–8,10–16], only HAMVECs exhibit this property in the absence of gelled basement membrane extract (**Fig. 3**) – albeit after a longer duration in co-culture with ASCs (**Supplementary Fig. 3**), presumably due to the need for the cells to secrete their own native extracellular matrix. Nevertheless, the self-assembly of ASCs into microvascular-like networks on gelled basement membrane extract may therefore be attributed to the composition of the substrate rather than their endothelial phenotype. Rich in laminin, collagen IV, and nidogen, the composition of gelled basement membrane extract (e.g. Matrigel®, Corning and Cultrex™, Bio-Techne) reflects that of the endothelial basement membrane, which normally separates ECs from underlying mural cells (i.e. pericytes and vascular smooth muscle cells) [39,40]. Accordingly, the self-assembly of ASCs in gelled basement membrane extract may in fact be a manifestation of their perivascular phenotype, recapitulating their predisposition to assume an abluminal localization to the endothelial basement membrane.

The endothelial basement membrane is critical to the stabilization and maturation of the endothelium [39,40]. Merely 20–200 nm thick, this specialized extracellular matrix upon which the endothelium resides is composed of laminin, collagen IV, nidogen, and heparin sulfate proteoglycans such as perlecan and agrin [39,40]. While these basement membrane constituents are predominantly produced by HAMVECs, our findings suggest that ASCs may contribute to the assembly of the basement membrane, at least in part, through their deposition of certain laminins and collagen IV (**Fig. 2**). These findings are in accordance with the current understanding of endothelial basement membrane biology [39,40], adding further support to the emergent role for mural cells in its assembly [41].

It is important to note, however, that ASCs are not a homogeneous population of mural cells. At least two distinct subpopulations of $CD45^{-}CD31^{-}$ ASCs reside within adipose tissue: $CD45^{-}CD31^{-}CD34^{-}$ ASCs and $CD45^{-}CD31^{-}CD34^{+}$ ASCs (**Fig. 1**). The localization of these cells *in situ* suggest that they comprise mural cells and stromal cells, respectively [42]. Furthermore, only a small proportion of ASCs exhibit well-defined αSMA filaments when co-cultured with HAMVECs, and these cells are found in close proximity to the vasculature – particularly at their branches (**Fig. 3**) – which is typical of pericytes [41]. However, it is unclear whether this disparate αSMA expression is a manifestation of the heterogeneous composition of ASCs and the self-organization of its constituent mural cells and stromal cells; the differentiation of ASCs towards a mural cell-like phenotype induced by paracrine and juxtacrine stimulation by proximal HAMVECs; or, a combination of both. Nevertheless, the findings of this investigation support previous observations of the perivascular phenotype of ASCs and their capacity to support HAMVECs [19–21].

ECs exhibit marked heterogeneity in order to address the distinct needs of the different vessels and tissues they service [4,23]. This phenotypic heterogeneity is most readily manifested by their arterial-venous specification and macrovascular-microvascular origin [43]. Accordingly, the proteomes of HAMVECs and ASCs were compared to EC controls representative of these predominant endothelial specializations, namely HUVECs (macrovascular, venous endothelium), HCAECs (macrovascular, arterial endothelium), and HDMVECs (microvascular endothelium). While HAMVECs share a similar proteome with these ECs – especially when juxtaposed with the proteome of ASCs – their principal component analysis and unsupervised hierarchical clustering underscored the distinct protein expression profiles that readily distinguish these different types of ECs (**Fig. 2**). Our findings complement previous observations that ECs retain distinct gene expression profiles despite their removal from their local milieu and culture under identical conditions [43], suggesting that effort should be directed at tailoring the phenotypic specialization of ECs to any given vascular tissue engineering application.

Notably, HUVECs exhibited the most distinctive proteome of the ECs derived from the four different vascular beds (**Fig. 2**). While venous endothelium is the predominant site of leukocyte extravasation during inflammation [23], HUVECs exhibit lower levels of immune markers – particularly those implicated in processing and presenting self-antigen (**Fig. 2**). Accordingly, the distinctive proteome of HUVECs may be a manifestation of their neonatal origin rather than venous specification, where suppressed self-antigen presentation may be a fetal mechanism associated with evading the maternal immune system [44]. It is important to note, however, that ASCs also exhibit lower abundances of these proteins (**Fig. 2**), and it is insufficient in enabling their long-term evasion of the immune system when used allogeneically [45]. Thus, given that most patients do not have an umbilical vein from which these cells can be autologously sourced, the implications of the distinct phenotype of neonatal HUVECs when compared with that of adult ECs warrants consideration by the biomaterials and vascular tissue engineering communities, for whom HUVECs have been the model EC of choice (use reported in ~ 60% of publications as of 2018) [46,47].

HAMVECs exhibited lower abundances of proteins involved in translation when compared with the other ECs (**Fig. 2**), which may be a manifestation of their slower rate of proliferation [18]. Nevertheless, the abundant and uniquely dispensable nature of fat mitigates the need for their extensive culture-mediated expansion, suggesting that this isn't a major limitation on their utility for vascular tissue engineering – for which the fundamental functions of the endothelium are to maintain blood in a fluid state and to confine its flow to the boundaries of the vessels. In fact, despite their phenotypic heterogeneity between vascular beds, all ECs express comparable levels of proteins responsible for regulating hemostasis and permeability (**Fig. 2**). This supports the utility of HAMVECs for the vascularization of engineered tissues [3] and the endothelialization of small diameter vascular prostheses [24]. Moreover, microvascular ECs exhibit arterial-venous-lymphatic specification [48], suggesting that HAMVECs isolated on the basis of the pan-endothelial marker CD31 may be further enriched for desirable phenotypic specifications and tailored to vascular tissue engineering applications, such as the endothelialization of small diameter vascular prostheses with ECs of an arterial specification to prevent their accelerated atherosclerotic disease progression [24].

Conclusion

Adipose tissue is an abundant, accessible, and uniquely dispensable source of cells for vascular tissue engineering. While considerable effort is still being directed at deriving endothelium from its resident stem and progenitor cells, our findings support the strikingly limited endothelial plasticity of ASCs and challenge the hypothesized persistence of developmentally conserved EPCs within fat. Rather, the current study supports the use of HAMVECs for the vascularization of engineered tissues and the endothelialization of small diameter vascular prostheses. The utility of ASCs for vascular tissue engineering appears to lie in their capacity to remodel the extracellular matrix and to function as mural cells. Our findings suggest that ASCs may stabilize and mature the endothelium, in part, by facilitating the assembly of its basement membrane. The work now warrants further investigation into the paracrine and juxtacrine interactions between HAMVECs and ASCs, and calls for exploration of the putative heterogeneity of HAMVECs (i.e. arterial, ve-

nous, and lymphatic subpopulations) and ASCs (i.e. stromal and mural subpopulations) to realize the full potential of fat for tissue engineering.

Declaration of Competing Interests

The authors declare that they have no known competing financial interests or personal relationships that could have appeared to influence the work reported in this paper.

Acknowledgements

The authors thank Kate Butler for her assistance in facilitating the provision of tissue for this research. This work was funded by the Canadian Institutes for Health Research (grant no. 230762 & 426275).

Supplementary materials

Supplementary material associated with this article can be found, in the online version, at doi:10.1016/j.bbiosy.2022.100049.

References

[1] Wu S, Coombs DM, Gurunian R. Liposuction: concepts, safety, and techniques in body-contouring surgery. Cleve Clin J Med 2020;87:367–75.
[2] Gir P, et al. Fat grafting: evidence-based review on autologous fat harvesting, processing, reinjection, and storage. Plast Reconstr Surg 2012;130:249–58.
[3] Rouwkema J, Khademhosseini A. Vascularization and angiogenesis in tissue engineering: beyond creating static networks. Trends Biotechnol 2016;34:733–45.
[4] Krüger-Genge A, Blocki A, Franke R, Jung F. Vascular endothelial cell biology: an update. Int J Mol Sci 2019;20:4411.
[5] Amerion M, Valojerdi MR, Abroun S, Totonchi M. Long term culture and differentiation of endothelial progenitor like cells from rat adipose derived stem cells. Cytotechnology 2018;70:397–413.
[6] Cheng F, et al. Conversion of human adipose-derived stem cells into functional and expandable endothelial-like cells for cell-based therapies. Stem Cell Res Ther 2018;9:350.
[7] Shi Z, Neoh KG, Kang ET, Poh CK, Wang W. Enhanced endothelial differentiation of adipose-derived stem cells by substrate nanotopography. J Tissue Eng Regen Med 2014;8:50–8.
[8] Qiu X, et al. Enhancement of endothelial differentiation of adipose derived mesenchymal stem cells by a three-dimensional culture system of microwell. Biomaterials 2015;53:600–8.
[9] Wang Z, et al. Osteogenic and angiogenic lineage differentiated adipose-derived stem cells for bone regeneration of calvarial defects in rabbits. *J Biomed Mater Res - Part A* 2021;109A:538–50.
[10] Shang T, et al. Hypoxia promotes differentiation of adipose-derived stem cells into endothelial cells through demethylation of ephrinB2. Stem Cell Res Ther 2019;10:133.
[11] Harris WM, et al. Endothelial differentiated adipose-derived stem cells improvement of survival and neovascularization in fat transplantation. Aesthetic Surg J 2019;39:220–32.
[12] Hsueh Y, et al. Synergy of endothelial and neural progenitor cells from adipose-derived stem cells to preserve neurovascular structures in rat hypoxic-ischemic brain injury. Sci. Rep. 2016;5:14985.
[13] Pham PV, Vu NB, Nguyen HT, Phan NK. Isolation of endothelial progenitor cells from human adipose tissue. Biomed Res Ther 2016;3:645–52.
[14] Forghani A, et al. Differentiation of adipose tissue–derived CD34+/CD31− cells into endothelial cells in vitro. Regen Eng Transl Med 2020;6:101–10.
[15] Froehlich H, Simari RD, Boilson BA. Differential phenotype and behavior in culture of CD34 positive cells from peripheral blood and adipose tissue. Heliyon 2021;7:e07779.
[16] Zhang P, et al. Endothelial differentiation of adipose-derived stem cells from elderly patients with cardiovascular disease. Stem Cells Dev 2011;20:977–88.
[17] Szklanny AA, et al. 3D bioprinting of engineered tissue flaps with hierarchical vessel networks (VesselNet) for direct host-to-implant perfusion. Adv Mater 2021;33:2102661.
[18] Antonyshyn JA, et al. Mitigating the non-specific uptake of immunomagnetic microparticles enables the extraction of endothelium from human fat. Commun Biol 2021;4:1205.
[19] Freiman A, et al. Adipose-derived endothelial and mesenchymal stem cells enhance vascular network formation on three-dimensional constructs in vitro. Stem Cell Res. Ther. 2016;7:5.
[20] Freiman A, et al. Engineering vascularized flaps using adipose-derived microvascular endothelial cells and mesenchymal stem cells. J Tissue Eng Regen Med 2018;12:e130–41.
[21] Redenski I, et al. Microcomputed tomography-based analysis of neovascularization within bioengineered vascularized tissues. ACS Biomater Sci Eng 2022;8:232–41.
[22] Antonyshyn JA, McFadden MJ, Gramolini AO, Hofer SOP, Santerre JP. Limited endothelial plasticity of mesenchymal stem cells revealed by quantitative phenotypic comparisons to representative endothelial cell controls. Stem Cells Transl Med 2019;8:35–45.
[23] Aird WC. Phenotypic heterogeneity of the endothelium: I. structure, function, and mechanisms. Circ Res 2007;100:158–73.
[24] Antonyshyn JA, D'Costa KA, Santerre JP. Advancing tissue-engineered vascular grafts via their endothelialization and mechanical conditioning. J Cardiovasc Surg (Torino). 2020;61:555–76.
[25] Cox J, et al. Andromeda: a peptide search engine integrated into the MaxQuant environment. J Proteome Res 2011;10:1794–805.
[26] Tyanova S, et al. The Perseus computational platform for comprehensive analysis of (prote)omics data. Nat Methods 2016;13:731–40.
[27] Cox J, et al. Accurate proteome-wide label-free quantification by delayed normalization and maximal peptide ratio extraction, termed MaxLFQ. Mol Cell Proteomics 2014;13:2513–26.
[28] Lex A, Gehlenborg N, Strobelt H, Vuillemot R, Pfister H. UpSet: visualization of intersecting sets. IEEE Trans Vis. Comput Graph. 2014;20:1983–92.
[29] Conway JR, Lex A, Gehlenborg N. UpSetR: an R package for the visualization of intersecting sets and their properties. Bioinformatics 2017;33:2938–40.
[30] Bonnot T, Gillard MB, Nagel DH. A simple protocol for informative visualization of enriched gene ontology terms. Bio-101 2019;9:e3429.
[31] Mi H, et al. PANTHER version 16: a revised family classification, tree-based classification tool, enhancer regions and extensive API. Nucleic Acids Res 2021;49:D394–403.
[32] Supek F, Bošnjak M, Škunca N, Šmuc T. REVIGO summarizes and visualizes long lists of gene ontology terms. PLoS One 2011;6:e21800.
[33] Arnaoutova I, Kleinman HK. In vitro angiogenesis: endothelial cell tube formation on gelled basement membrane extract. Nat Protoc 2010;5:628–35.
[34] Schindelin J, et al. Fiji: An open-source platform for biological-image analysis. Nat Methods 2012;9:676–82.
[35] Nishikawa SI, Nishikawa S, Hirashima M, Matsuyoshi N, Kodama H. Progressive lineage analysis by cell sorting and culture identifies FLK1+VE-cadherin+ cells at a diverging point of endothelial and hemopoietic lineages. Development 1998;125:1747–57.
[36] Hirashima M, Kataoka H, Nishikawa S, Matsuyoshi N, Nishikawa SI. Maturation of embryonic stem cells into endothelial cells in an in vitro model of vasculogenesis. Blood 1999;93:1253–63.
[37] Yamashita J, et al. Flk1-positive cells derived from embryonic stem cells serve as vascular progenitors. Nature 2000;408:92–6.
[38] Carmeliet P. Mechanisms of angiogenesis and arteriogenesis. Nat Med. 2000;6:389–95.
[39] Davis GE, Senger DR. Endothelial extracellular matrix: biosynthesis, remodeling, and functions during vascular morphogenesis and neovessel stabilization. Circ Res 2005;97:1093–107.
[40] Lau S, Gossen M, Lendlein A. Designing cardiovascular implants taking in view the endothelial basement membrane. Int J Mol Sci 2021;22:13120.
[41] Armulik A, Genové G, Betsholtz C. Pericytes: developmental, physiological, and pathological perspectives, problems, and promises. Dev Cell 2011;21:193–215.
[42] Zimmerlin L, et al. Stromal vascular progenitors in adult human adipose tissue. Cytom Part A 2010;77A:22–30.
[43] Chi JT, et al. Endothelial cell diversity revealed by global expression profiling. Proc Natl Acad. Sci. USA. 2003;100:10623–8.
[44] Niederkorn JY. See no evil, hear no evil, do no evil: the lessons of immune privilege. Nat Immunol 2006;7:354–9.
[45] Ankrum JA, Ong JF, Karp JM. Mesenchymal stem cells: immune evasive, not immune privileged. Nat Biotechnol 2014;32:252–60.
[46] Hauser S, Jung F, Pietzsch J. Human endothelial cell models in biomaterial research. Trends Biotechnol 2017;35:265–77.
[47] Wang K, Lin R, Melero-Martin JM. Bioengineering human vascular networks: trends and directions in endothelial and perivascular cell sources. Cell Mol Life Sci 2019;76:421–39.
[48] Potente M, Mäkinen T. Vascular heterogeneity and specialization in development and disease. Nat Rev Mol Cell Biol 2017;18:477–94.